Science Advances
AAAS

Supplementary Materials for

Similar but different: Characterization of *dddD* gene–mediated DMSP metabolism among coral-associated *Endozoicomonas*

Yu-Jing Chiou *et al.*

Corresponding author: Sen-Lin Tang, sltang@gate.sinica.edu.tw

Sci. Adv. **9**, eadk1910 (2023)
DOI: 10.1126/sciadv.adk1910

This PDF file includes:

Auxiliary Supplementary Materials

Supplementary Results
Detailed genomic features of of *Ca.* E. ruthgatesiae 8E

The 8E genome contained 88 tRNA and 22 rRNA genes, including 8 5S rRNA, 7 16S rRNA, and 7 23S rRNA genes (table. S2). Seven 16S rRNA genes separated into 2 subclades in the phylogenetic tree. A similarity test was performed for all the 16S rRNA copies of 8E using local blast. A discrepancy was found in one copy of the 16S rRNA gene which showed lower identity with other copies (identity > 97.7 %). Despite some variations between the genes, these genes were still clustered in a single clade by the phylogenetic analysis (Fig. 1E). In the genome of 8E, a total of 5229 CDSs were annotated, and no prophage was detected. Only 1452 CDSs were classified into RAST subsystems, which is fewer than other known *Endozoicomonas* type strains indicated the discrepancy with other known bacteria. Like the previous functional report of the genus *Endozoicomonas* (*2*), we found that the most abundant subsystem was Amino Acids and Derivatives (282), followed by Protein Metabolism (227), Cofactors, Vitamins, Prosthetic groups, Pigments (138), and Carbohydrates (135) (fig. S8a). Like other *Endozoicomonas* in RAST subsystem profiles, 8E displayed a high portion of genes classified in Amino Acids and Derivatives (19.8 %), Protein Metabolism (15.9%), and Carbohydrates (9.51%) (fig. S8a). 8E have the most genes categorized in Protein Metabolism out of all *Endozoicomonas*, especially in protein biosynthesis and protein folding (fig. S8c).

8E had 33 gene copies of chromosome segregation ATPases (SMC superfamily) and 16 gene copies of chromosome segregation proteins (SMC prok B superfamily), which might relate to cell division and the structural maintenance of chromosomes, respectively. Chromosome segregation proteins and ATPases are common in bacteria, and all *Endozoicomonas* species contain multiple copies of them. Based on the phylogenetic tree of the two proteins, we confirmed that the 8E chromosome segregation protein and ATPase were separated from the protein sequences of other *Endozoicomonas* and formed a discrete clade (fig. S2c, d). We found 6 copies of glycosyltransferase (Gly transf sug superfamily), which might functionally catalyze the glycosidic linkages synthesis, scattered in the 2.74–2.97 Mbps region. There was a high density of various sized DNA TRs (1,126 TRs) ranging from 30 to 2,000 bp in 8E, mostly located at 4.94 – 5.07Mbp (74 TRs) and 5.84–6.31Mbp (361 TRs).

Description of the *Endozoicomonas ruthgatesiae* sp. nov

Endozoicomonas ruthgatesiae (ru.th.gates'iae, N.L. fem. n. ruthgatesiae, of Ruth Gates, name of a coral biologist). Cells are Gram-negative, aerobic, and rod shape with 0.4-0.8 μm wide, and 1.6-4.0 μm long. No mobility was observed but flagella-like structures and fimbriae-like structures were observed in the minimal medium with 0.1mM DMSP (Fig. 2B). After incubation on Mmbv4 agar at 25 ℃, colonies are beige, crateriform, and circular with undulate margin. The colony size is around 0.6mm in diameter incubated for 3 days at 25 ℃. Sodium ions are required for growth; grow in 0.5-4.0 % NaCl. Growth occurs at 20-35 ℃ (optimum, 25℃), and pH 6-9 (optimum, 7). Oxidase and Catalase activity are strong. In API ZYM kit test, except for alkaline phosphatase, esterase, lipase, leucine arylamidase, valine arylamidase, cystine arylamidase, trypsin, and acid phosphatase, others are negative. *Ca.* E. ruthgatesiae exhibited no activity for α-chymotrypsin, α-galactosidase, β-galactosidase, β-glucuronidase, β-glucosidase, N-acetyl- β-glucosaminidase, α- mannosidase, and α-fucosidase. In addition to the above negative enzymatic activities, *Ca*. E. ruthgatesiae had no Naphthol-AS-BI-phosphohydrolase activity, but this activity was detected in other species of *Endozoicomonas* (table S1).

Bacterial colony are moderately susceptible to streptomycin (10 µg/ml) and ampicillin (10 µg/ml). The current strain is 8E. isolated from coral *Acropora* sp. collected from Kenting, Pingtung, Taiwan. (Coral collection procedures in Kenting National Park were permitted by Kenting, Pingtung County Government with permit number No. 10670917900). To honor the dedication of Professor Dr. Ruth Gates to coral reefs, we name the de novo coral isolated bacterium: *Endozoicomonas ruthgatesiae.*

Supplementary Discussion
High proportion of eukaryotic-like proteins in 8E

ELPs originated from eukaryotes and horizontally transferred to the associated prokaryotes. Their functions are mostly hypothesized to relate to bacterial-host interactions (*61*). ELPs are now commonly detected in bacterial genomes. *Endozoicomonas* is one of bacterial groups which often carry ELPs (*11*, *12*, *14*, *62*) However, different *Endozoicomonas* clades possess distinct ELPs that might be caused by various adaptation strategies in symbiosis construction with their coral hosts (*63*). In this study, we found that the total 8E genome consisted of more than 8% ELPs, which is more than the other *Endozoicomonas* genomes used in our comparative genomic analysis (fig. S2). Similar phenomenon were also purported in a recent study which annotated a tremendous amount of ELPs (1/3 of putative ELPs) in an *Acropora humilis* isolated *E. marisrubri* 6c, 7.69 Mb genome (*14*). The great deal of ELPs is likely one of the reasons for the genome expansion in 8E and the other large *Endozoicomonas* genomes, despite the absence of prophage and plasmids. The large amount of ELPs in coral associated *Endozoicomonas* suggests that *Endozociomonas* species might have broad host ranges for different coral species or have coevolved with various coral hosts over time. However, what the specific functions of these ELPs are, and why these ELPs are largely expanded with multiple copies in the large *Endozoicomonas* genomes, are still unanswered and intriguing questions.

WD40 domain proteins and Ankyrin repeats are the two major ELPs in *Endozoicomonas* genomes. The functions of ankyrin repeats have been proposed variously in different bacteria. For instance, in the sponge *Cymbastela cencentrica* symbiont, ankyrin repeats may help bacteria avoid phagocytosis by the predator amoeba (*64*) but, in human microphages, ankyrin repeats are used to assist host-cell gene modulation (*65*). Recently, WD40 proteins in prokaryotes have gained more attention (*66-68*) but their abundance is usually less than 1 % in bacterial genomes, and most of them are reported from *Cyanobacteria* and *Planctomycetes* (*68*). The WD40 domain was first described in association with cellular functions in eukaryotes(*69*) In prokaryotes the WD40 proteins are mostly annotated as serine/threonine protein kinase and participate in biological processes or functions, such as ribosome assembly and transmembrane proteins(*70*). Interestingly, WD40 proteins are the most abundant ELPs in the 8E genome, accounting for around 3% with 160 copies. The high number of WD40 proteins comprise various domains which are typically composed of 7 to 16 repeating units. These variations in the domains result in various protein functions with different physical and chemical properties (*64*). Notably, the abundance of WD40 proteins are proposed to be positively related with genome size(*70*). A similar phenomenon can be found in the larger *Endozoicomonas* genomes (> 7Mb) (This study and (*14*)), not in the smaller *Endozoicomonas* genomes. We herein propose ELPs play a key factor in *Endozoicomonas*-coral host interactions and encourage more studies, especially on their cellular and physiological functions. These studies will be helpful in gaining insights into molecular interactions in coral and other organism holobionts.

Supplementary Methods

Morphological characterization

For colony morphological observation, the bacteria were separated by four ways streaking on 1.5% agar and 0.1% glucose MMB medium and incubated for 4 days for single colony formation at the fourth region. The single colony was observed using a dissecting microscope (Leica E45, Germany).

For microscopic characterization, log-phase bacterial cells were collected, and the medium was replaced by PBS to reduce the background non-target signal before adding a fixative buffer (2.5% glutaraldehyde + 4 % paraformaldehyde/0.1M PBS) at 37 °C for 10 min. For bacterial morphology observation, cells were mounted on grow-discharge carbon-formvar grids and stained by 2% phosphotungstate for 1 s, and immediately rinsed by sterilized H_2O. For inner cell structural characterizations, fix bacterial cells were then centrifuged at 4500 rpm for 5 min, and the bacterial pellets were fixed in 2.5 % glutaraldehyde and 4 % paraformaldehyde in 0.1 M sodium phosphate buffer, pH 7.0 at room temperature for 1 hour. After three 20 min buffer rinses, the samples were post-fixed in 1% OsO4 in the same buffer for 1 hour at room temperature and then rinsed in three 20 min changes of buffer. Samples were dehydrated in an alcohol series, embedded in Spurr's resin, and sectioned with a Leica Reichert Ultracut S or Leica EM UC6 ultramicrotome. The ultra-thin sections (70–90 nm) were stained with 5% uranyl acetate in 50% methanol and 0.4% lead citrate in 0.1 N sodium hydroxide. General bacterial cell morphology and bacterial cell ultra-thin sections were both observed using a FEI G2 Tecnai Spirit Twin transmission electron microscope at 80 KV, and the images were taken with a Gatan Orius CCD camera.

Except for the cell morphology grown in broth medium, we also observed the cell morphology grown on agar. 8E was first grown on a Mmbv4 agar plate with 0.1% glucose for 5 days, 1 mm × 1 mm agars with few single colonies were cut and loaded on the medium-containing stub, then frozen by liquid nitrogen slush. The frozen sample was transferred to the sample preparation chamber at -160℃. After 5 minutes, the temperature was raised to -85℃, and the samples were etched for 20 minutes. After coating at -130℃, the samples were transferred to the SEM chamber and observed at -160℃ and 20KV using a cryo scanning electron microscope (FEI Quanta 200 SEM/Quorum Cryo System PP2000TR FEI).

Physiological and biochemical characteristics

Bacterial mobility was determined by stabbing a bacterial inoculum into the center of a semi-solid MMB medium (0.5% agarose) and then observing for the diffuse zone of bacterial growth in the agar tube. The Gram stain kit (Fluka, England) was used to differentiate the gram-positive or -negative bacteria. To reveal the optimal growth characteristics of the newly isolated bacterium (i.e., 8E) at specific pH, temperature, and salinity, bacteria at the log phase were used for all the tests. The concentration of the bacteria was determined by spectrophotometry. A wavelength of 600 nm was used to measure bacterial concentration (Analytik Jena ScanDrop 250, Germany). For the tests, bacteria were cultivated in seven different pH media from pH 4, 5, 6, 7, 8, 9 and 10; seven different salinity media with 0, 0.5, 1, 2, 3, 4, 5% of NaCl; and nine different temperature conditions, 10, 15, 20, 25, 28, 30, 33, 35, 40 ℃. An API 20NE kit (bioMérieux, France) was used to reveal biochemical characteristics of the bacterium. Tolerance to low oxygen was tested by culturing 8E for 10 days in a 2.5 L Oxoid AnaeroGen (Thermo, USA) sealed jar system with a carbon dioxide produced sachet for anaerobic environment generation. Activity of catalase (35 % H_2O_2) and oxidase test (0.1% tetramethyl-p--phenylenediamine dihydrochloride, TMPD) were examined independently by dropping the prepared solution on the smear bacterial culture directly.

Genome annotation and characteristics of *Ca.* E. ruthgatesiae 8E

tRNA and rRNA genes were predicted by Aragorn (*71*) and Barrnap (*72*) respectively, and coding sequences (CDS) were predicted by Prodigal. The three tools mentioned above were integrated in Prokka v 1.14.6 (*73*). The annotation was completed using the default settings in Prokka. To facilitate the comparison between 8E and other *Endozoicomonas* species, the functional gene categories were classified by RAST (Rapid Annotation using Subsystems Technology) (Aziz et al., 2008) (*74*) and visualized by the SEED viewer (*75*). Putative bacteriophages in bacterial genomes were identified using PHASTER (*76*), and only prophages marked as "intact" were recorded. WD40 domain protein and ankyrin repeat protein were specifically annotated using NCBI Batch web CD search using the conserved domain database (CDD) v3.19 (*77*) with e-value < 0.001 and a maximum number of hits = 10. Tandem repeats were annotated by Tandem Repeats Finder (TRF) v4.09 (*78*) with a maximum period size of 2000 bp. EffectiveELD 5.2 in EffectiveDB (*79*) was used to predict the number of eukaryotic-like domains and eukaryotic-like domains secreted proteins with a minimum score of 4.

Delineation of genomic taxonomy

To analyze the phylogenetic relationship of 8E in the genus *Endozoicomonas*, all sequences were first aligned using cmalign, a covariance model (CM) aligner included in the Infernal package (*80*). The bacterial domain of the CM was obtained from the Rfam database (*81*). A maximum likelihood tree was constructed using IQ-Tree v.2.2.0-beta (*58*) with 1000 replicates of bootstraps analysis, and the best model, Blosum62+F+I+G4, was chosen by ModelFinder (*82*). A consensus tree was generated by iqtree (*83*) and visualized on iTOL (*84*) UBCGs (Up-to-date bacterial core gene sets) (*85*) were used to concatenate and align 92 core genes to further confirm the position of 8E in the family *Endozoicomonadaceae*. ANI and AAI were calculated using the "ANI/AAI-matrix calculator" (*86*) and heatmaps were generated from R (*87*) using the pheatmap (*88*) package.

***Endozoicomonas* genome comparison and visualization**

The first base of the assembled genome of 8E was determined using the gene, *dnaA*, by Seqkit (*89*). A genomic atlas was generated by CG-View (*90*) and compared with other *Endozoicomonas* genome by the BLASTn +2.12 with 0.001 expect value. Low identity regions were manually checked by the Mauve rearrangement reviewer (*91*). The proteins in low identity regions were picked and compared with other *Endozoicomonas* by phylogenetic tree construction. Protein sequences were aligned by MAFFT version 7 (*92*) and consensus trees were built and visualized using the same tool described before.

RNA extraction sequencing and gene expression analysis

The total RNAs were extracted using TRIzoI reagent (Invitrogen, Thermo Fisher Scientific, MA, USA) and followed procedures described in the manufacturer's instruction. Briefly, 1 mL TRIzoI solution was added to the sample tube. Samples were mixed thoroughly by vortexing for 30 s and incubated at room temperature for 5 mins. Phase separation was performed with centrifugation (12,000 x *g*) at 4°C for 10 min. The upper aqueous phase was transferred to a fresh tube. Then, 200 µl of chloroform was added to the sample tube, which was then incubated at room temperature for 10 mins. Phase separation was performed again under the same condition. The upper aqueous phase was transferred to a new tube and mixed with 500 µl isopropanol. After the phase separation step (12,000 x *g* at 4°C for 8 mins), the supernatant was discarded. Then, 75% ethanol was used for washing the pellet twice. After removing the ethanol by centrifuge, the RNA pellet was air dried and dissolved in nuclease-free water. Then, the RNA product was quantitated using a Qubit RNA HS Assay kit and Qubit fluorometer, according to the

manufacturer's instructions. The RNA integrity number (RIN) for each sample was measured using Bioanalyzer 2100 (Agilent, USA). In the end, RNA-seq libraries were subjected to Illumina sequencing on a HiSeq2500 (paired-end) at the NGS High Throughput Genomics Core of Biodiversity Research Center in Academia Sinica, Taiwan.

Reads were first quality checked by FastQC (*93*), and mapped onto the 8E genome using Bowtie 2 (*94*). FeatureCounts (*95*) was used to assign reads to genomic features. To compare the transcriptomic expression between treatment (DMSP addition) and control (without DMSP addition), the DESeq2 package (*96*) in R was used to normalize reads and generate Log fold changes on gene expression levels. Two different conditions of two DMSP degraders were compared: 8E (1) 0 hr control vs. 6 hr control, (2) 6 hr control vs. 6 hr treatment; and *E. acroproae* (1) 0 hr control vs. 8 hr control, (2) 8 hr control vs. 8 hr treatment. Pathway prediction was done using the web based BlastKOALA (*97*) and the gene was manually picked up for heatmap classification using the package pheatmap (*88*) in R.

DMSP and DMS calibration curve

We used two different mediums for the assay and prepared two calibrations, one for each of the mediums, to avoid unexpected ingredients affecting the efficiency of alkaline lysis of the DMSP in the supernatant. Five DMSP standards were prepared (minimal medium: 0.025 mM, 0.05 mM, 0.1 mM, 0.15 mM, 0. 2mM) (MMB: 0.025 mM, 0.05 mM, 0.1 mM, 0.25 mM, 0.5 mM), and 1 mL of each was added to a 20 mL sealed vial with 0.1mL 5M NaOH (alkaline lyase), respectively, and incubated in the dark at 25 ℃ , 200 rpm for 30 min. After that, 500 µl of headspace gas was extracted using a gastight syringe and injected manually into GC (using the same program mentioned above). The peak area was collected for the calibration curve, and each concentration had three replicates.

For DMS gas quantification, two ranges of calibration curves (2.8-14ppm, 80-400 ppm) were prepared. For making two distinct ranges of DMS concentration, 1 and 2 µl of 99.9% DMS (MW;62.130, 0.864 g/cm^3) liquid were extracted using a micro-gastight syringe and injected into a 1200- and 500-ml serum bottle, respectively. The 80 ℃ heated ovens were prepared for complete evaporation of DMS, and the serum bottles were kept in the oven before sample extraction. To create five concentration gradients, different volumes (low concentration: 0.01 ml, 0.025 ml, 0.040 ml, 0.060 ml, 0.080 ml; high concentration: 0.06 ml, 0.12 ml, 0.18 ml, 0.24 ml, and 0.3 ml) were used. The injection procedure was the same as previously mentioned. DMS concentration was calculated using the following equation $DMS_{(^{mg}/_{m^3})} =$

$[DMS_{(extraction\ volum\ \mu l)} \times DMS_{density(kg/L)} \times (^{L}/_{10^6 \mu l}) \times (^{10^6 mg}/_{kg})]/$

$[serum\ bottle\ volume_{(ml)} \times (^{m^3}/_{10^6 ml})$.

Not all DMS cleavage by bacteria was released from the medium to the headspace. Hence, the dissolved DMS has been estimated and depends on the Bunsen solubility coefficient (β_T) using the protocol developed by S. Hamilton in 2006. In this calculation, we assumed the salinity of the medium was negligible, and the barometric pressure was 1 in the experiment vessel whose headspace volume was 0.2 L, and liquid volume was 0.1 L at 25 ℃.

8E distribution around the Indo-Pacific region

Four different coral microbial community studies were included for the 8E distribution analysis: first, a bacterial community study focused on *Acropora muricata* in Taiwan, Okinawa and Kochi published from our lab (*98*) second and third, studies that collected coral microbial communities in West Australia (*99*)and the Davies Reef (*100*) and fourth, a study which targeted two different coral species in the Red Sea, *A. hemprichii* and *Pocillopora verrucosa.* All 16S

microbial amplicon raw sequences were downloaded from NCBI and had the amplicon primers removed by QIIME2 (*101*) cutadapt function. We denoised the sequences using DADA2 binding in QIIME2 and removed rare ASVs with read counts less than 2, then assigned taxonomy. Similarity searches were performed on all ASV sequences collected from four different studies against 7 copies of 8E 16S rRNA sequences with local blastn. Only the ASVs that fit the criteria "identity $\geq$ 99%, e-value $<$ 1e-5, mismatch and gaps $\leq$ 3 " could be identified as 8E. The map was drawn using R (*102*), ggplot2 (*103*) package.

Supplementary figures and tables

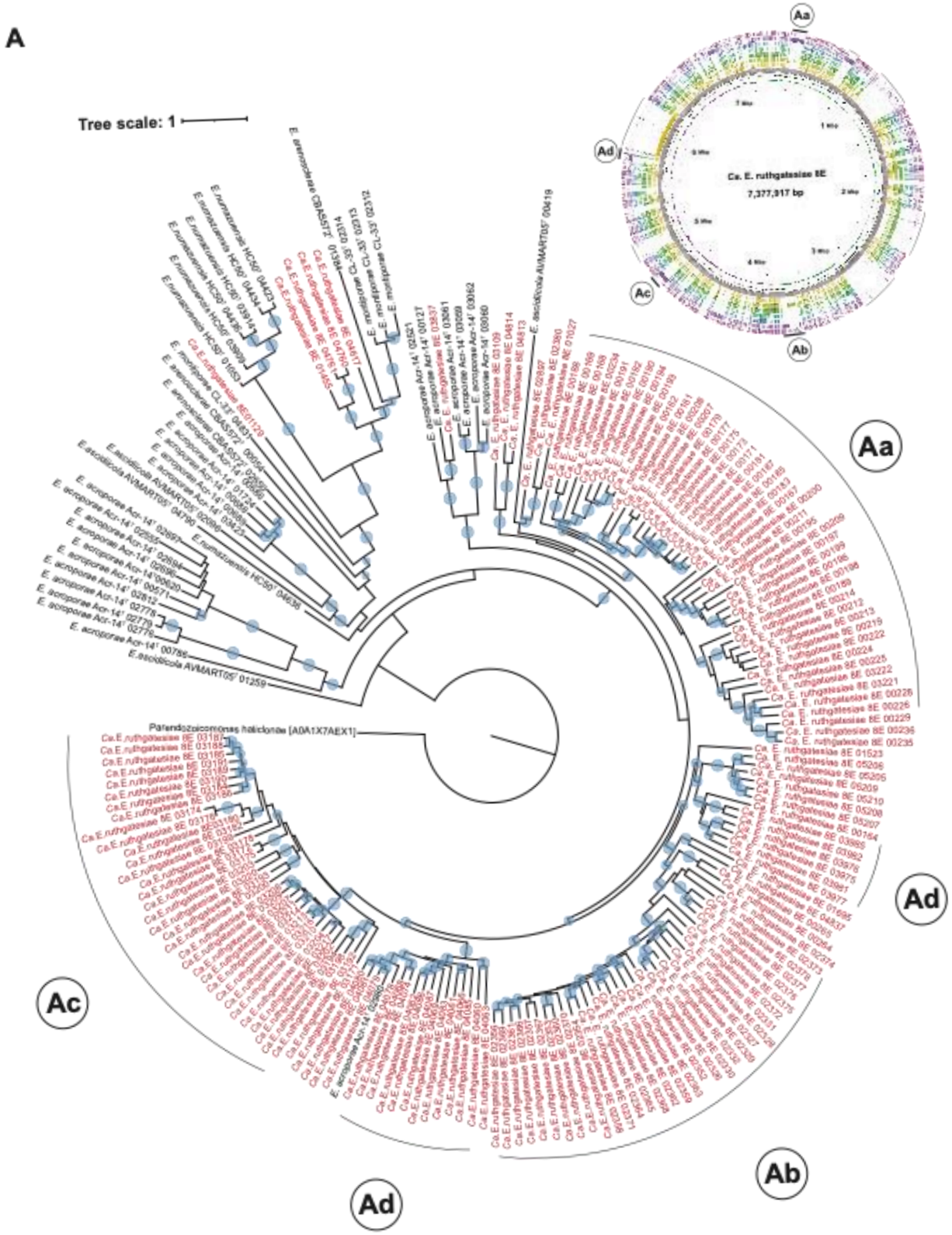
A
Tree scale: 1
Aa
Ab
Ac
Ad
Ca. E. ruthgatesiae 8E
7,377,917 bp
Parendozoicomonas haliclonae [A0A1X7AEX1]

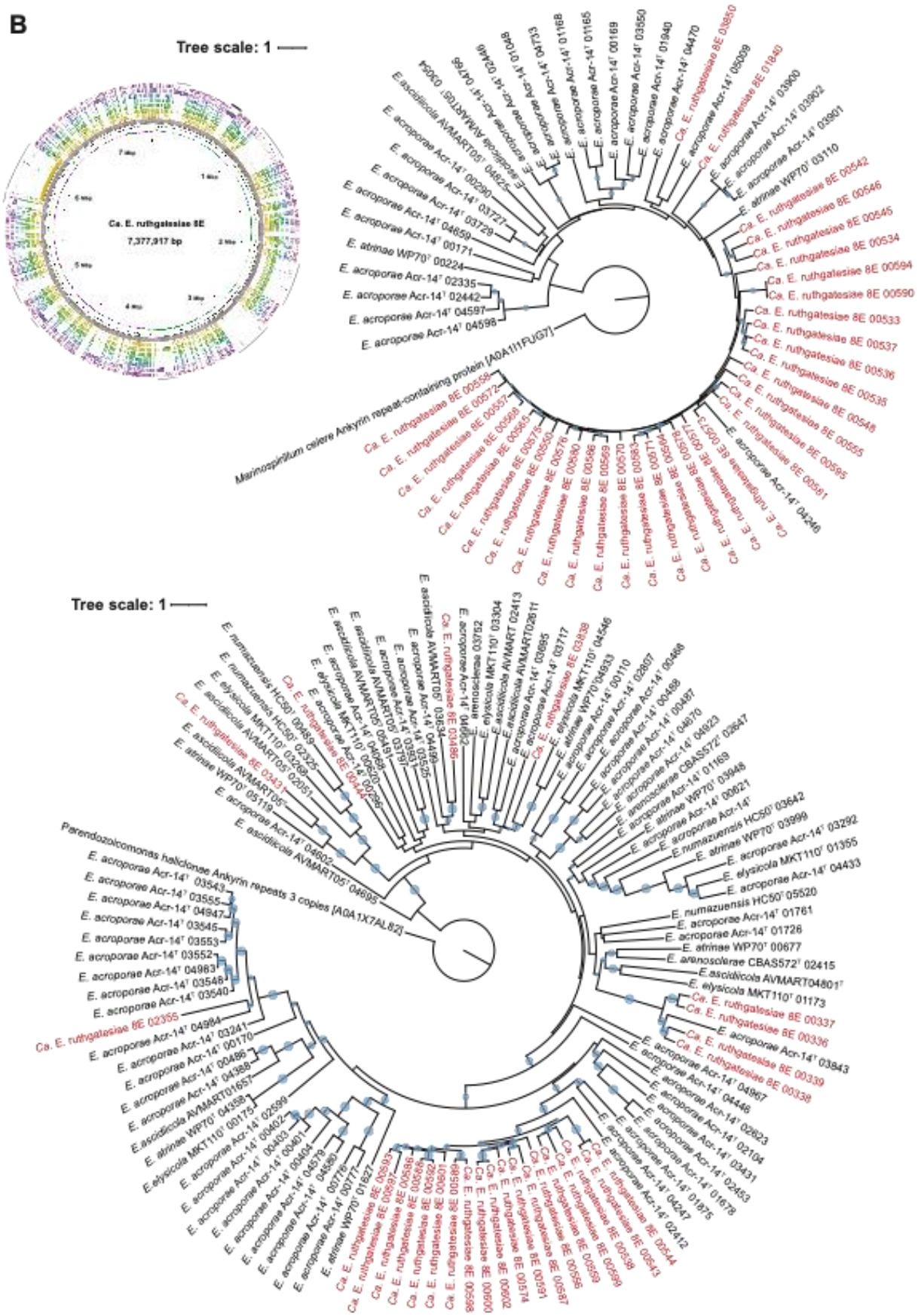
B
Tree scale: 1
Ca. E. ruthgatesiae 8E
7,377,917 bp
Marinospirillum celere Ankyrin repeat-containing protein [A0A1I1FUG7]
Tree scale: 1
Parendozoicomonas haliclonae Ankyrin repeats 3 copies [A0A1X7AL82]

C

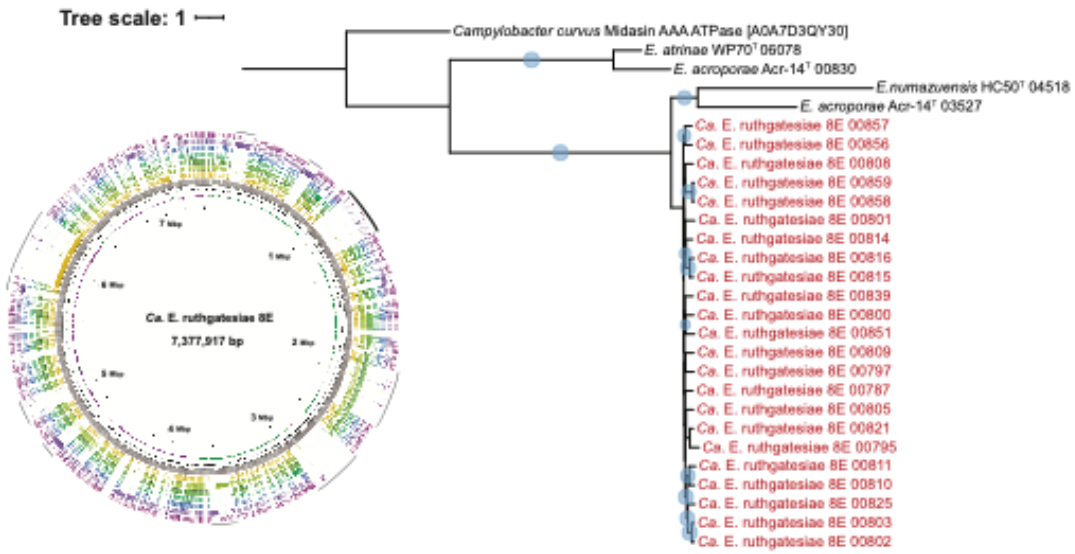
Tree scale: 1
Campylobacter curvus Midasin AAA ATPase [A0A7D3QY30]
E. atrinae WP70T 06078
E. acroporae Acr-14T 00830
E.numazuvensis HC50T 04518
E. acroporae Acr-14T 03527
Ca. E. ruthgatesiae 8E 00857
Ca. E. ruthgatesiae 8E 00856
Ca. E. ruthgatesiae 8E 00808
Ca. E. ruthgatesiae 8E 00859
Ca. E. ruthgatesiae 8E 00858
Ca. E. ruthgatesiae 8E 00801
Ca. E. ruthgatesiae 8E 00814
Ca. E. ruthgatesiae 8E 00816
Ca. E. ruthgatesiae 8E 00815
Ca. E. ruthgatesiae 8E 00839
Ca. E. ruthgatesiae 8E 00800
Ca. E. ruthgatesiae 8E 00851
Ca. E. ruthgatesiae 8E 00809
Ca. E. ruthgatesiae 8E 00797
Ca. E. ruthgatesiae 8E 00787
Ca. E. ruthgatesiae 8E 00805
Ca. E. ruthgatesiae 8E 00821
Ca. E. ruthgatesiae 8E 00795
Ca. E. ruthgatesiae 8E 00811
Ca. E. ruthgatesiae 8E 00810
Ca. E. ruthgatesiae 8E 00825
Ca. E. ruthgatesiae 8E 00803
Ca. E. ruthgatesiae 8E 00802
Ca. E. ruthgatesiae 8E
7,377,917 bp

fig. S1 Phylogenetic tree of identical characteristics of 8E and other *Endozoicomonas* species. (A) WD40 repeat. 160 WD40 domain proteins have been annotated and separated to four different regions in the 8E genome. There are 47 WD40 proteins scattered from around 0.197Mbp to 0.331Mbp (Aa), 34 proteins at around 3.49Mbp to 3.64Mbp (Ab), 38 proteins from 4.62Mbp to 4.78Mbp (Ac), and 23 proteins from around 5.50Mbp to 5.79Mbp (Ad). The relative location is marked on the upper 8E genome. **(B) Ankyrin repeats.** 66 ankyrin repeats have been annotated and 56 are of ankyrin repeat containing proteins, and ankyrin repeats (3 copies) mix at around 0.436Mbp to 0.744Mbp. The relative location is marked as 2 on the 8E genome. (**C) Midasin AAA ATPase.** The 23 proteins located at around 0.966Mbp to 1.23Mbp, marked as 3 on the 8E genome**.** The relative location is marked as 5 on the upper 8E genome. The outgroups of *Parendozoicomonas haliclonae* WD40 protein, ankyrin repeats (3 copies), *Marinospirillum celere* Ankyrin repeat-containing protein, *Campylobacter curvus* Midasin AAA ATPase, *Thalassolituus oleivorans* chromosome segregation protein was all obtained from UniProtKB and include accession numbers at the end. Multiple protein sequences were inferred from the MAFFT alignment, after that maximum likelihood tree were calculated by iqtree with 1,000 replications. The minimum bootstrap values were 80 and marked with a light blue circle on the branching points of the trees.

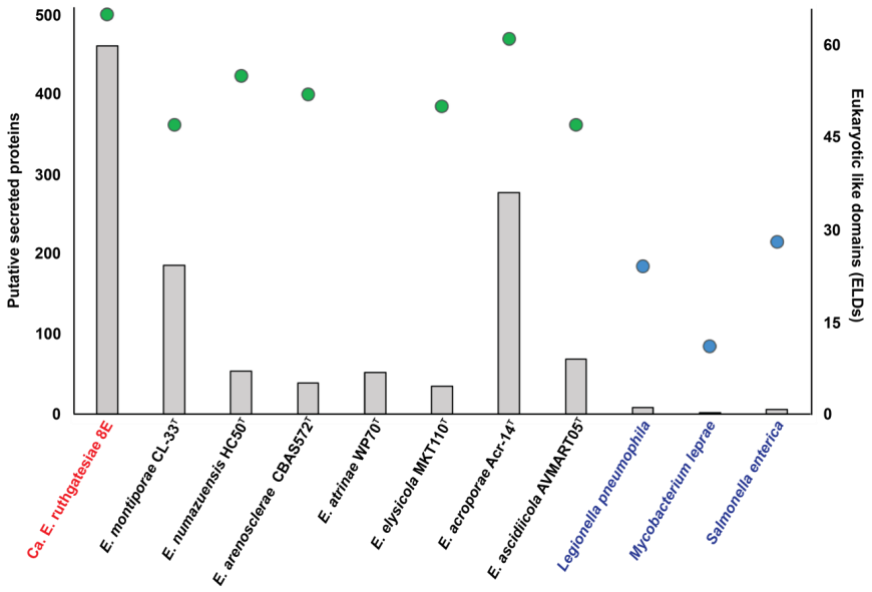

fig. S2 The number of eukaryotic like domain and putative secreted protein in *Endozoicomonas* species and obligate symbiotic bacteria.

The bar chart shows the number of high score secreted proteins annotated by EffectiveELD with minimal ELD score > 4. Green spots belong to *Endozoicomonas* species and blue spots are obligate symbiotic bacteria. The input protein sequences were annotated by Prokka v1.14.6 and the original genome files, except *Ca*. E. ruthgatesiae, were obtained from the NCBI database (table S4).

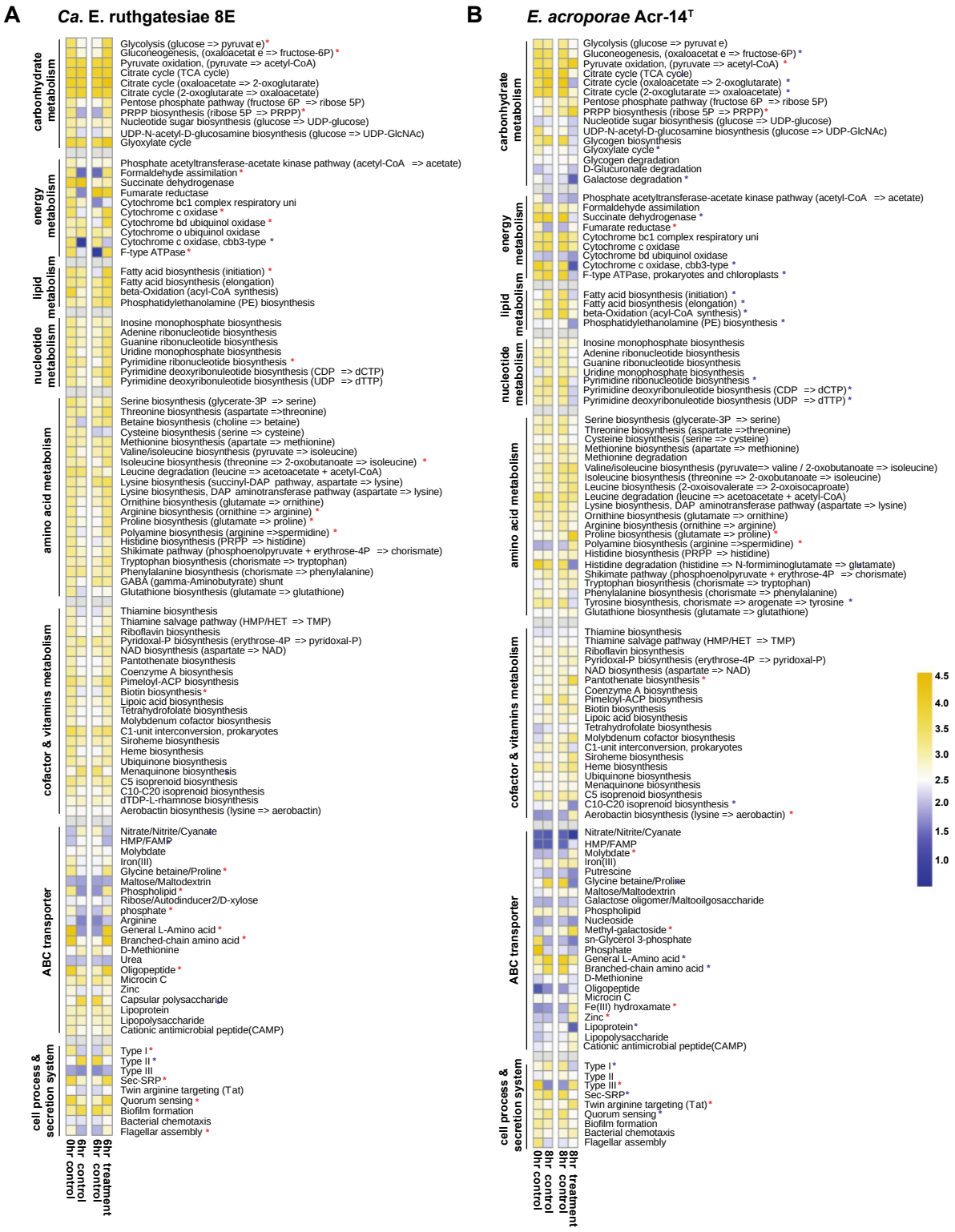

fig. S3 The heatmap of the overall pathway based on the average normalized count. Raw read was normalized by DESeq2 and on average all genes participated in the specific pathway according to the KEGG annotation. A red star indicates that the differences of normalized count are 10 times more in the 6hr/8hr treatment than in the 6hr/8hr control, and a blue star indicates the opposite. The numbers on the color bar correspond to the logarithm of normalized counts. **(A) *Ca.* E. ruthgatesiae 8E overall pathway heatmap. (B) *E. acroporae* Acr-14^{T} overall pathway heatmap.** The left two columns are the control (without DMSP), and the right column is the treatment (with DMSP).

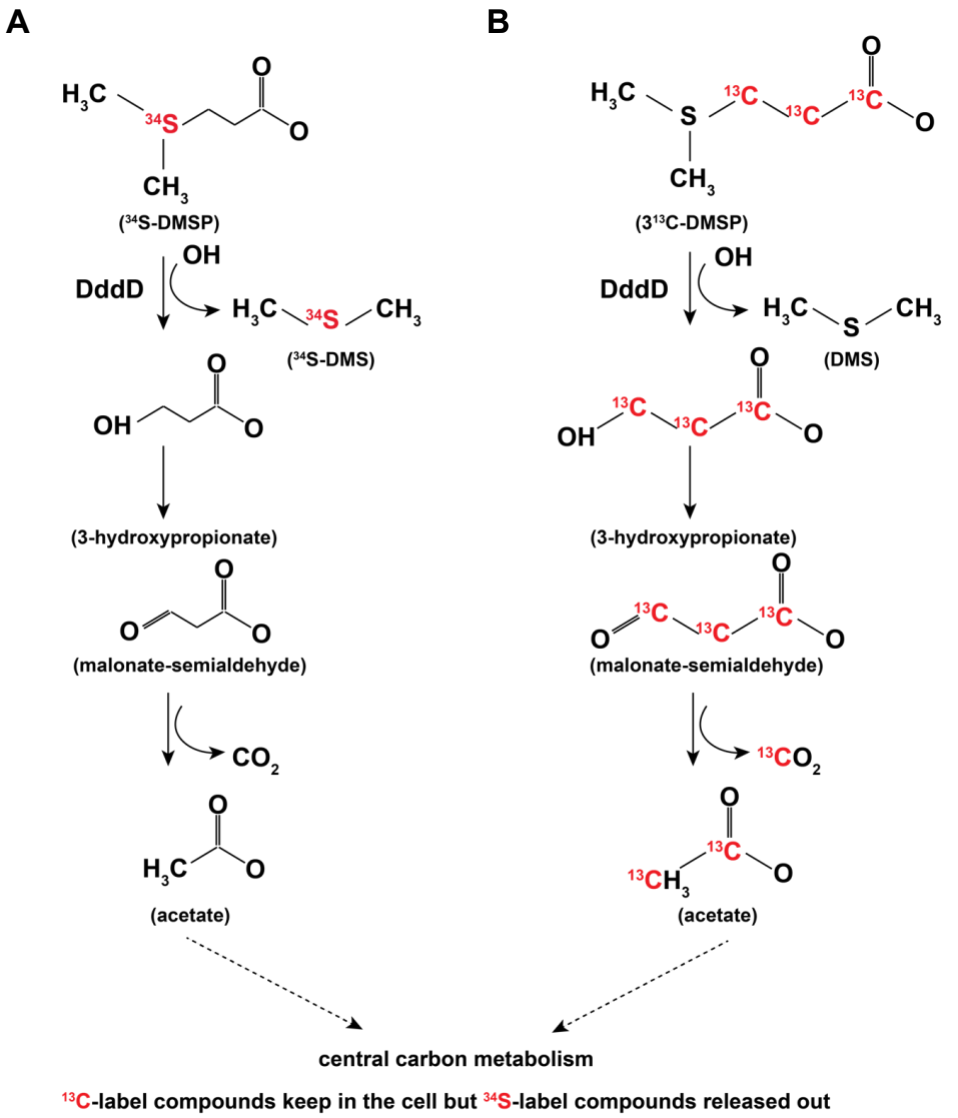

fig. S4 The expected stable isotope – label DddD based DMSP metabolic pathway.
(A) ^{34}S-label position on the DMSP and the tracer metabolic expected pathway. ^{34}S was expected to be released out of the cells along with the DMS production. **(B) 3 ^{13}C-label position on the DMSP and the tracer expected metabolic pathway.** One ^{13}C label compound was expected to be released through carbon dioxide, while the other two ^{13}C label-compounds were expected to stay in the cell and participate in the bacterial central carbon metabolism.

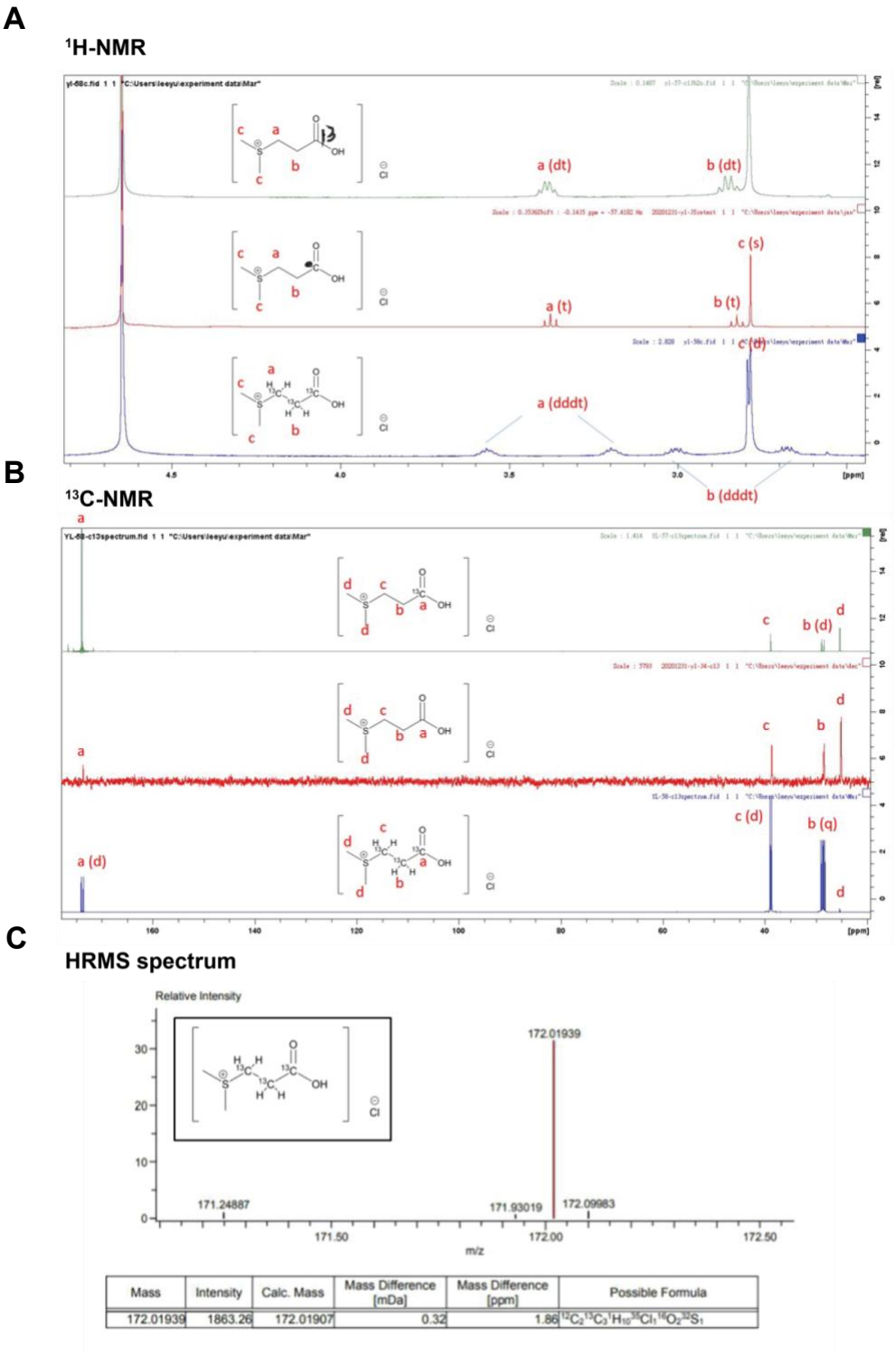

Mass	Intensity	Calc. Mass	Mass Difference [mDa]	Mass Difference [ppm]	Possible Formula
172.01939	1863.26	172.01907	0.32	1.86	$^{12}C_2{}^{13}C_3{}^{1}H_{10}{}^{35}Cl_1{}^{16}O_2{}^{32}S_1$

fig. S5 NMR and HRMS spectrum of stable isotopic labelled DMSP.
(A) ^{1}H-NMR spectrum. a: [1-^{13}C] DMSP; b: DMSP; and c: [1,2,3-$^{13}C_3$] DMSP**. (B) ^{13}C-NMR.** a; [1-^{13}C] DMSP, b; DMSP, and c; [1,2,3-$^{13}C_3$] DMSP. **(C) HRMS spectrum of [1,2,3-$^{13}C_3$] DMSP.**

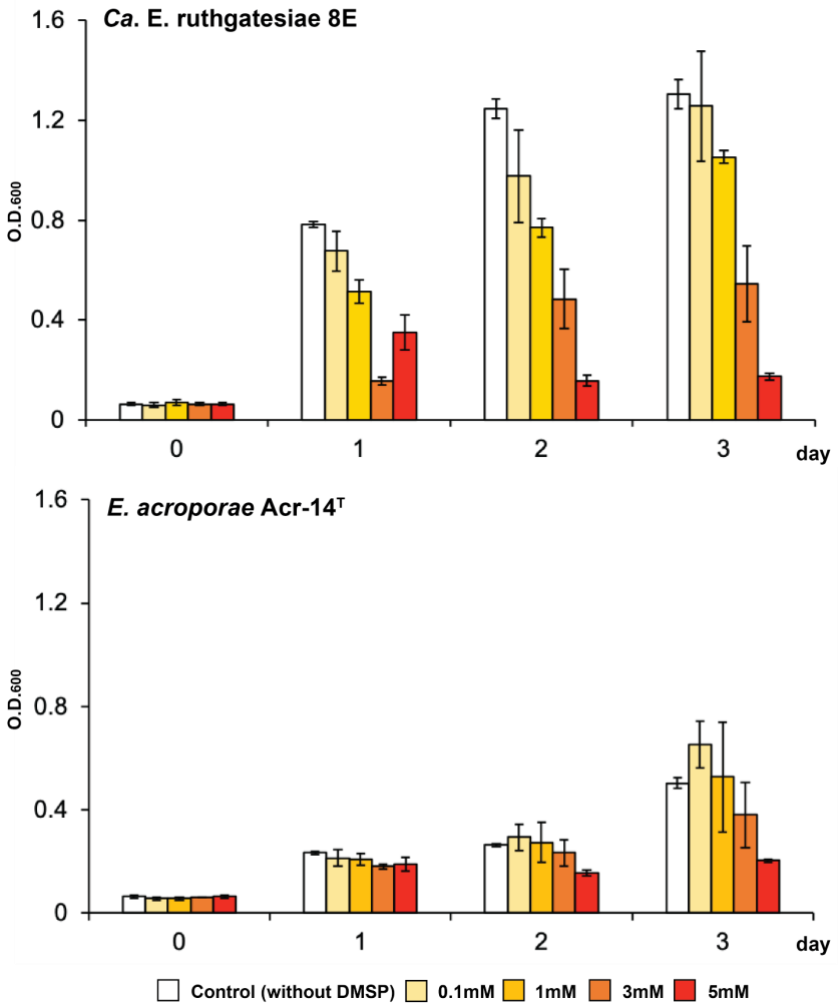

fig. S6 The DMSP dose-dependent assay of two *Endozoicomonas* species.
The assay was performed to detect bacterial proliferation with different concentrations of DMSP. Each treatment with a specific DMSP concentration has three replicates. Control samples are minimum medium/0.2% casamino acid added only; test samples were treated with different concentrations (i.e., 0.1 mM, 1.0 mM, 3.0 mM, and 5 mM) of DMSP in minimum medium/ 0.2% casamino acid added.

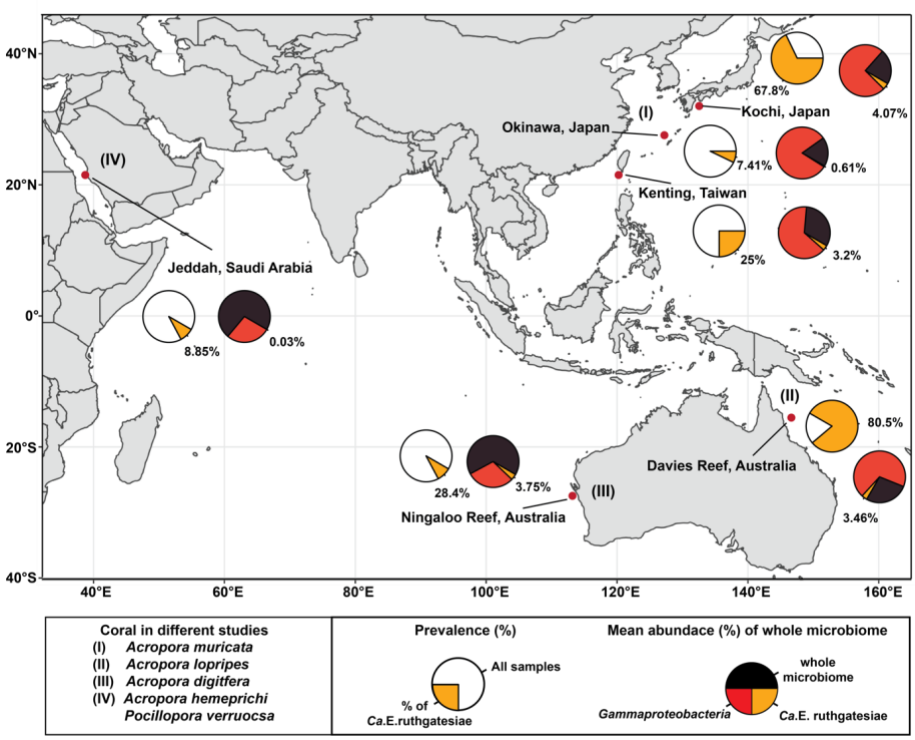

fig. S7 *Ca*. E. ruthgatesiae prevalence and abundance around the Indo-Pacific Ocean.
Four studies were included for amplicon sequence variant (ASV) analysis, and a similarity search was performed by including and comparing all ASVs against *Ca*. E. ruthgatesiae 16S rRNA gene sequences with local blastn. The yellow region in one pie chart represents the prevalence of *Ca*. E. ruthgatesiae in all samples of the study, and in the other pie chart, represents the mean abundance of the whole microbiome (identified at identity ≥99%, e-value < 1e-5, and mismatch & gap ≤3).

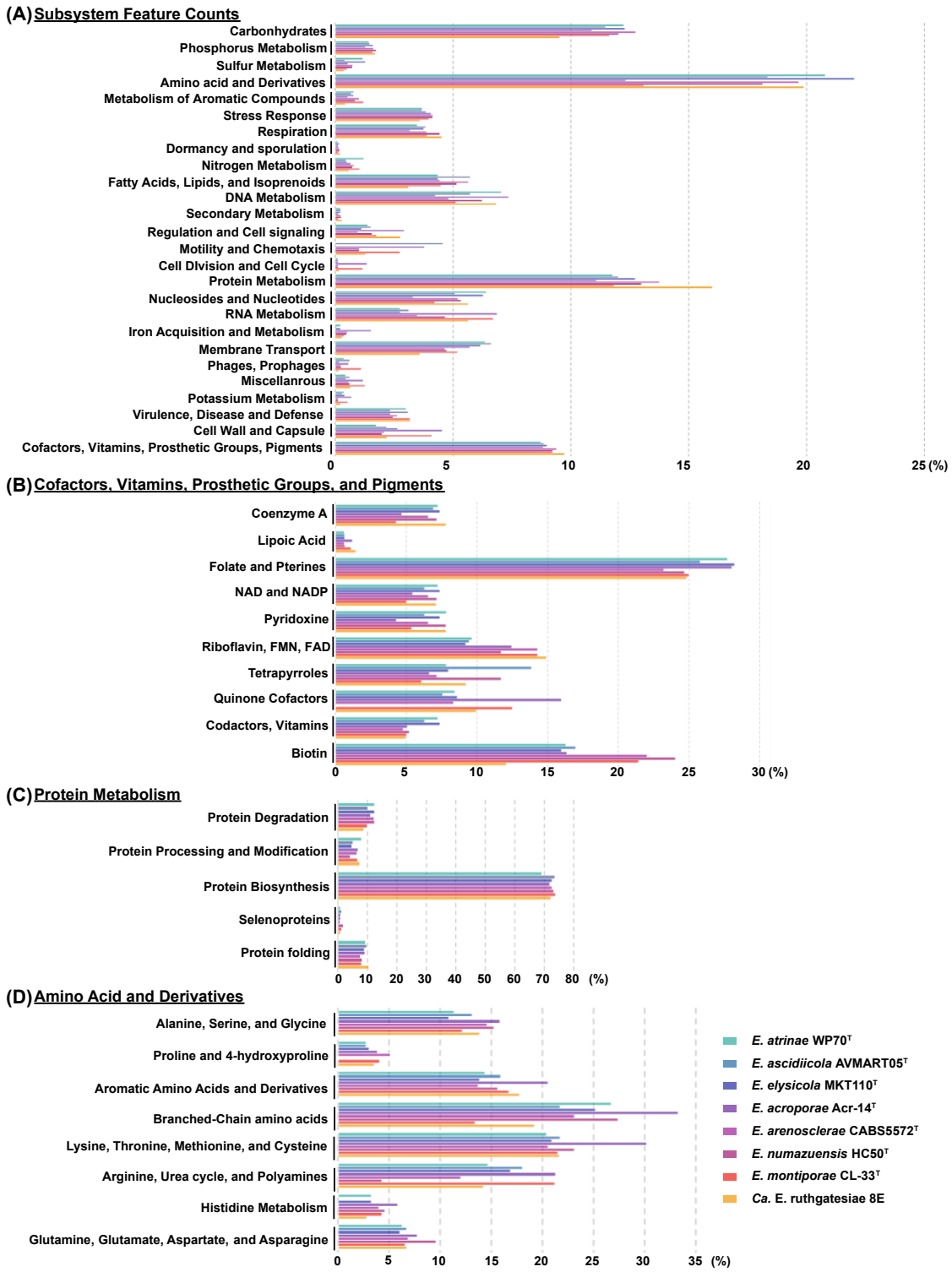

fig. S8 *Endozoicomonas* species functional annotation by RAST tool kit (*RASTtk*).
(A) RAST subsystem feature distribution, showing percentage of annotated genes in each feature. (B) Percentage of genes related to Cofactors, Vitamins, Prosthetic Groups, and Pigments. (C) Percentage of genes related to Protein metabolism. (D) Percentage of genes related to Amino acid and derivates.

table S1, Differential phenotypic characteristics of *Candidatus* Endozoicomonas ruthgatesiae and other *Endozoicomonas* species.

Characteristics	*Ca.* E.ruthgatesiae 8E (This study)	*E. montiporae* CL-33^{T*}	*E. numuensis* HC50^{T*}	*E. arenosclerae* CBAS572^{T*}	*E. atrinae* WP70^{T*}	*E. elysicola* MKT110^{T*}	*E. acroporae* Acr-14^{T*}	*E. ascidiicola* AVMART05^{T*}
Isolated source	Hexacoral	Hexacoral	Marine sponge	Marine sponge	Comb pen shell	Sea slug	Hexacoral	Ascidians
Colony pigment (medium)	Beige	Beige#	Pale creamy White/yellowish brown #	Cream#	Beige #	Beige #	Cream white#	Margins#
Cell size (µm)	1.6-4.0 ×0.4-0.8	1.0-3.0 × 0.5-0.7	3.0-10 × 0.4-0.8	0.5-1.0 (diameter)	0.7-1.0×1.2-3.6	0.4-0.6 ×1.8-2.2	2.0 - 3.0 × 0.5 -0.8	0.3-0.7×1.2-11.3
Relation to O_2	A	A	FAN	A	A	A	A	FAN
Motility	−	+	−	+	−	+	−	+
Catalase activity	+	+	+	ND	+	+	+	+
Oxidase activity	+	+	+	ND	+	+	+	+
Optimum /Growth temperature	25 /20-35	25 /15-35	25 /15-37	20-30 /12-35	30 /15-37	25-30 /4.0-37	30/ 20-35	23 /5-27
Optimum / Growth pH	7.0 /6.0-9.0	8.0 /6.0-10	7.5-8.0 /5.5-9.0	ND	7.0 /6.0-9.0	ND	7.0 /5.0-10	6.0-7.0 /6.2-8.3
Optimum /Growth NaCl (PSU)	10,20 /5-40	20 /10-50	20 /10-50	30 /20-50	20 /10-40	> 0 /> 0	20/10-50	1.0 /0.5-5.0
Alkaline phosphatase	+	+	+	+**	+	ND	+	+
Esterase	+	−	+	−**	+	ND	+	+
Lipase	+	−	+	−	−	ND	+	−
Leucine arylamidase	+	+	+	ND	+	ND	+	+
Valine arylamidase	+	−	+	ND	+	ND	+	+
Cystine arylamidase	+	−	−	ND	−	ND	+	−
Trypsin	+	−	−	ND	+	ND	−	+
α-chymotrypsin	−	−	−	ND	−	ND	−	−
Acid phosphatase	+	+	+	ND	+	ND	+	
Naphthol-AS-BI-phosphohydrolase	−	+	+	ND	+	ND	+	+
α-galactosidase	−	−	−	ND	+	ND	−	−
β-galactosidase	−	−	−	−**	+	ND	−	−
β-glucuronidase	−	−	−	ND	+	ND	−	−
β-glucosidase	−	−	−	−	−	ND	−	−
N-acetyl-β-glucosaminidase	−	−	−	+**	+	ND	−	+
α-mannosidase	−	−	−	ND	−	ND	−	−
α-fucosidase	−	−	−	ND	−	ND	−	−

** phenotypic data obtained from genomic sequences. # Bacterial colonies were growth on Marine agar.

table S2, ***Endozoicomonas*** **genome characteristics**

Endozoicomonas **strains**	**Genome assembly size (Mb)**	**Contig N50 (bp)**	**contigs**	**GC content (%)**	**CDS**	**rRNA**	**tRNA**	**Prophage**	**WD40 domain protein**	**Ankyrin repeat protein**	**DddD**
***Ca*. E. ruthgatesie 8E**	**7.37 (99.14)**	**7,377,917**	**1**	**48**	**5229**	**22**	**88**	**0**	**160**	**66**	+
E. acroporae **Acr-14^{T}**	6.05 (98.56)	47,658	309	49.2	4,821	18	78	1	23	97	+
E. acroporae **Acr-1$^{\#}$**	6.03 (98.99)	56,565	299	49.3	4,872	6	77	3	22	97	+
E. acroporae **Acr-5$^{\#}$**	6.03 (98.99)	58,040	295	49.3	4,872	7	80	3	22	97	+
E. montiporae **CL-33^{T}**	5.43 (98.99)	1,612,341	3	48.5	4,808	22	114	2	4	1	–
E. arenosclerae **CBAS572^{T}**	6.45 (99.14)	44,889	328	47.0	5,614	25	118	1	3	4	–
E. ascidiicola **AVMART05^{T}**	6.51 (97.63)	42,432	300	46.0	5650	16	73	1	4	13	–
E. atrinae **WP70^{T}**	6.68 (98.92)	21,158	985	47.1	4,880	15	81	0	0	10	–
E. elysicola **MKT110^{T}**	5.61 (98.98)	481,336	21	46.8	4,526	21	85	0	0	8	–
E. numazuensis **HC50$^{T\#}$**	6.34 (99.14)	124,905	131	47.1	5,177	9	90	1	7	6	–
Endozoicomonas **sp. SM1973$^{\#}$**	6.82 (99.78)	99,815	597	40.0	6,029	2	59	0	1	10	–
Endozoicomonas **sp. G2-1$^{\#}$**	4.12 (99.21)	233,877	46.05	42.5	3,734	5	83	0	1	1	+
Endozoicomonas **sp. AB1**	4.04 (94.85)	20,472	284	46.0	3,376	2	42	ND	ND	ND	–
Parendozoicomonas haliclonae	5.46 (99.57)	458,274	69	51.5	4.645	7	98	ND	ND	ND	–
Kistimonas asteriae	5.01(99.57)	199,845	49	51.4	4,289	8	93	ND	ND	ND	–

table. S3. The DddD protein identity of *Ca*. E. ruthgatesiae and other DddD-containing *Gammaproteobacteria*

	Ca. E. ruthgatesiae (%)
Endozoicomonas sp. YOMI1	93.182
Endozoicomonas sp. ONNA1	92.703
Marinobacter zhejiangensis [SFM33971.1]	75.866
Pseudomonas sp. SJZ079 [TWC34159.1]	75.598
Marinobacter mobilis [SDX71985.1]	75.747
Marinobacter sp. JH2 [QBM19223.1]	74.791
Amphritea atlantica [SER18761.1]	73.596
Pseudomonas guineae [SFI11272.1]	74.313
Pseudomonas sp. J465 [ACY01992.1]	74.910
Marinomonas aquiplantarum [RBO85988.1]	70.167
Marinomonas rhizomae [RBP79500.1]	69.809
Moritella sp. JT01 [KXO07111.1]	69.498
Marinomonas balearica [TDO98802.1]	69.056
Endozoicomonas sp. G2_1	67.900
Endozoicomonas acroporae Acr 1	68.225
Endozoicomonas acroporae Acr 5	68.225
Endozoicomonas acroporae Acr 14^{T}	68.225
Marinomonas pollencensis [REG86934.1]	66.428
Endozoicomonas sp. SESOKO1	68.176
Endozoicomonas sp. ONNA2	67.386
Marinomonas fungiae [CUB04494.1]	65.476
Grimontia indica [EOD79702.1]	62.127
Pseudomonas chlororaphis subsp. aureofaciens [AZD92653.1]	59.304
Pseudomonas putida [AMK30774.1]	59.259
Granulosicoccus antarcticus IMCC3135 [ASJ71256.1]	55.875
Halomonas sp. HTNK1 [ACV84065.1]	54.012
Psychrobacter sp. JB385 [SJN22021.1]	54.524
Psychrobacter sp. J466 [ACY02894.1]	52.758
Pseudomonas sp. NFR09 [SET63727.1]	42.788

table S4. Number of reads for Transcriptomic analysis at different stages

Ca. E. ruthgatesiae 8E									
Time points (hr)	0			6			6		
Treatments	Without DMSP			Without DMSP			With DMSP		
Replicate	1	2	3	1	2	3	1	2	3
QC check	13,441,846	12,022,407	11,485,312	11,088,084	10,537,288	11,910,898	10,443,195	11,449,719	13,983,154
Phred score	37.62	37.56	37.62	37.56	37.56	37.59	37.60	37.57	37.61
Mapping to bacterial genome (alignment rate %)	13,313,402 (99.04%)	11,894,683 (98.94%)	11,364,048 (98.94%)	10,975,052 (98.98%)	10,443,432 (99.11%)	11,786,988 (98.96%)	10,354,373 (99.15%)	11,347,671 (99.11%)	13,825,245 (98.87%)
Assigned to transcripts	12,194,899	10,919,295	10,448,497	10,248,524	9,645,204	10,849,819	9,569,331	10,439,729	12,698,793

E. acroporae Acr-14^{T}									
Time points (hr)	0			8			8		
Treatments	Without DMSP			Without DMSP			With DMSP		
Replicate	1	2	3	1	2	3	1	2	3
QC check	10,123,608	9,969,432	10,011,479	10,214,200	10,395,201	10,492,924	10,375,195	11,200,996	12,238,878
Phred score	37.49	37.46	37.48	37.52	37.50	37.58	37.57	37.56	37.55
Mapping to bacterial genome (alignment rate %)	10,017,887 (98.56%)	9,875,021 (98.42%)	9,843,561 (97.73%)	10,120,982 (98.56%)	10299898 (98.40%)	10,405,533 (98.70%)	10,276,746 (98.53%)	11,133,864 (98.70%)	12,072,400 (98.44%)
Assigned to transcripts	9,146,330	9,168,171	9,111,140	9,123,576	9,309,553	9,432,910	9,392,321	10,162,624	10,971,733

tableS5, Genome accession number obtained from NCBI used in this study.

Bacterial genome	GeneBank assembly accession
Endozoicomonas montiporae CL-33^T	GCA_001583435.1
Endozoicomona numazuensis HC50^T	GCA_000722635.1
Endozoicomona arenosclerae CBAS572^T	GCA_001562015.1
Endozoicomona atrinae WP70^T	GCA_001647025.2
Endozoicomona elysicola MKT110^T	GCA_000710775.1
Endozoicomona acroporae Acr-14^T	GCA_002864045.1
Endozoicomona acroporae Acr-1	GCA_010994335.1
Endozoicomona acroporae Acr-5	GCA_010994325.1
Endozoicomona ascidiicola AVMART05^T	GCA_001646955.1
Endozoicomona sp. AP1-3	CP114886
Endozoicomona sp. Tanguisson_1	CP114771
Endozoicomona sp. SM1973	GCA_013425485.1
Endozoicomona sp. G2_1	GCA_017744155.1
Endozoicomonas sp. AB1	GCA_001729985.1
Endozoicomonas sp. ONNA1	GCA_024606325.1
Endozoicomonas sp. YOMI1	GCA_024606345.1
Endozoicomonas sp. ONNA2	GCA_024606365.1
Endozoicomonas sp. SESOKO1	GCA_024606265.1
Parendozoicomonas haliclonae	GCA_900174585.1
Kistimonas asteriae	GCA_018263925.1
Legionella pneumophila	GCA_001753085.1
Mycobacterium leprae	GCF_001457695.1
Salmonella enterica	GCF_003718315.1

table S6. DMSP cleavage gene containing *Endozoicomonas*

***Endozoicomonas* species**	**DMSP cleavage gene**	**Coral Host**	**Completed operon**
Ca. E. ruthgatesiae (This study)	*dddD*	*Acropora* sp.	Yes
E. acorporae	*dddD*	*Acropora* sp.	Yes
Endozoicomonas sp. G2_1	*dddD*	*Acropora cyntherea*	Yes
Endozoicomonas sp. ONNA1	*dddD*	*Acropora tenuis*	Yes
Endozoicomonas sp. ONNA2	*dddD*	*Acropora tenuis*	No
Endozoicomonas sp. SESOKO1	*dddD*	*Acropora tenuis*	No
Endozoicomonas sp. YOMI1	*dddD*	*Acropora tenuis*	No
Endozoicomonas sp. AP1-3	*dddD*	*Acropora pulchra*	Yes
Endozoicomonas sp. Tanguisson_1	*dddD*	*Acropora pulchra*	Yes
E. 'pistillata' typeB	*dddP*	*Stylophra pistillata*	unknown

REFERENCES AND NOTES

1. S. Li, T. Young, S. Archer, K. Lee, S. Sharma, A. C. Alfaro, Mapping the green-lipped mussel (*Perna canaliculus*) Microbiome: A multi-tissue analysis of bacterial and fungal diversity. *Curr. Microbiol.* **79**, 76 (2022).

2. M. J. Neave, C. T. Michell, A. Apprill, C. R. Voolstra, Endozoicomonas genomes reveal functional adaptation and plasticity in bacterial strains symbiotically associated with diverse marine hosts. *Sci. Rep.* **7**, 40579 (2017).

3. M. Nishijima, K. Adachi, A. Katsuta, Y. Shizuri, K. Yamasato, *Endozoicomonas numazuensis* sp. nov., a gammaproteobacterium isolated from marine sponges, and emended description of the genus *Endozoicomonas* Kurahashi and Yokota 2007. *Int. J. Syst. Evol. Microbiol.* **63** (Pt 2), 709–714 (2013).

4. R. E. Pike, B. Haltli, R. G. Kerr, Description of *Endozoicomonas euniceicola* sp nov and *Endozoicomonas gorgoniicola* sp nov., bacteria isolated from the octocorals *Eunicea fusca* and *Plexaura* sp., and an emended description of the genus *Endozoicomonas*. *Int. J. Syst. Evol. Microbiol.* **63** (Pt 11), 4294–4302 (2013).

5. L. Schreiber, K. U. Kjeldsen, M. Obst, P. Funch, A. Schramm, Description of *Endozoicomonas ascidiicola* sp. nov., isolated from Scandinavian ascidians. *Syst. Appl. Microbiol.* **39**, 313–318 (2016).

6. S. Y. Sheu, K. R. Lin, M. Y. Hsu, D. S. Sheu, S. L. Tang, W. M. Chen, *Endozoicomonas acroporae* sp nov., isolated from *Acropora* coral. *Int. J. Syst. Evol. Microbiol.* **67**, 3791–3797 (2017).

7. J. L. Meyer, V. J. Paul, M. Teplitski, Community shifts in the surface microbiomes of the coral *Porites astreoides* with unusual lesions. *PLOS ONE* **9**, e100316 (2014).

8. K. M. Morrow, D. G. Bourne, C. Humphrey, E. S. Botté, P. Laffy, J. Zaneveld, S. Uthicke, K. E. Fabricius, N. S. Webster, Natural volcanic CO2 seeps reveal future trajectories for host–microbial associations in corals and sponges. *ISME J.* **9**, 894–908 (2015).

9. Z. Qin, K. Yu, S. Chen, B. Chen, Q. Yao, X. Yu, N. Pan, X. Wei, Significant changes in bacterial communities associated with *Pocillopora* corals ingestion by crown-of-thorns starfish: An important factor affecting the coral's health. *Microorganisms* **10**, 207 (2022).

10. M. J. Neave, C. T. Michell, A. Apprill, C. R. Voolstra, Whole-genome sequences of three symbiotic *Endozoicomonas* strains. *Genome Announc.* **2**, e00802–e00814 (2014).

11. K. Tandon, C.-Y. Lu, P.-W. Chiang, N. Wada, S.-H. Yang, Y.-F. Chan, P.-Y. Chen, H.-Y. Chang, Y.-J. Chiou, M.-S. Chou, W.-M. Chen, S.-L. Tang, Comparative genomics: Dominant coral-bacterium *Endozoicomonas acroporae* metabolizes dimethylsulfoniopropionate (DMSP). *ISME J.* **14**, 1290–1303 (2020).

12. J.-Y. Ding, J.-H. Shiu, W.-M. Chen, Y.-R. Chiang, S.-L. Tang, Genomic insight into the host–Endosymbiont relationship of *Endozoicomonas montiporae* CL-33^{T} with its coral host. *Front. Microbiol.* **7**, 251 (2016).

13. K. Tandon, Y.-J. Chiou, S.-P. Yu, H. J. Hsieh, C.-Y. Lu, M.-T. Hsu, P.-W. Chiang, H.-J. Chen, N. Wada, S.-L. Tang, Microbiome restructuring: Dominant coral bacterium *Endozoicomonas* species respond differentially to environmental changes. *mSystems* **7**, e0035922 (2022).

14. C. Pogoreutz, C. A. Oakley, N. Rädecker, A. Cárdenas, G. Perna, N. Xiang, L. Peng, S. K. Davy, D. K. Ngugi, C. R. Voolstra, Coral holobiont cues prime *Endozoicomonas* for a symbiotic lifestyle. *ISME J.*, **16**, 1883–1895 (2022).

15. L. M. Fitzgerald, A. M. Szmant, Biosynthesis of 'essential' amino acids by Scleractinian corals. *Biochem. J.* **322** (Pt 1), 213–221 (1997).

16. J.-B. Raina, D. Tapiolas, B. L. Willis, D. G. Bourne, Coral-associated bacteria and their role in the biogeochemical cycling of sulfur. *Appl. Environ. Microbiol.* **75**, 3492–3501 (2009).

17. E. Ransome, S. J. Rowley, S. Thomas, K. Tait, C. B. Munn, Disturbance to conserved bacterial communities in the cold-water gorgonian coral *Eunicella verrucosa*. *FEMS Microbiol. Ecol.* **90**, 404–416 (2014).

18. M. O. Andreae, Ocean-atmosphere interactions in the global biogeochemical sulfur cycle. *Mar. Chem.* **30**, 1–29 (1990).

19. G. Kirst, Osmotic adjustment in phytoplankton and macroalgae: The use of dimethylsulfoniopropionate (DMSP) In R. P. Kiene, P. T. Visscher, K. D. Maureen, G. Kirst, Eds. *Biological and environmental chemistry of DMSP and related sulfonium compounds.* (Plenum Press, 1996) pp. 121-129.

20. G. Kirst, C. Thiel, H. Wolff, J. Nothnagel, M. Wanzek, R. Ulmke, Dimethylsulfoniopropionate (DMSP) in icealgae and its possible biological role. *Mar. Chem.* **35**, 381–388 (1991).

21. A. M. Theseira, D. A. Nielsen, K. Petrou, Uptake of dimethylsulphoniopropionate (DMSP) reduces free reactive oxygen species (ROS) during late exponential growth in the diatom Thalassiosira weissflogii grown under three salinities. *Mar. Biol.* **167**, 127 (2020).

22. W. Sunda, D. Kieber, R. Kiene, S. Huntsman, An antioxidant function for DMSP and DMS in marine algae. *Nature* **418**, 317–320 (2002).

23. C. Aguilar, J.-B. Raina, C. A. Motti, S. Fôret, D. C. Hayward, B. Lapeyre, D. G. Bourne, D. J. Miller, Transcriptomic analysis of the response of *Acropora millepora* to hypo-osmotic stress provides insights into DMSP biosynthesis by corals. *BMC Genomics* **18**, 612 (2017).

24. S. G. Gardner, M. R. Nitschke, J. O'Brien, C. A. Motti, J. R. Seymour, P. J. Ralph, K. Petrou, J.-B. Raina, Increased DMSP availability during thermal stress influences DMSP-degrading bacteria in coral mucus. *Front. Mar. Sci.* **9**, 10.3389/fmars.2022.912862 (2022).

25. S. G. Gardner, D. A. Nielsen, O. Laczka, R. Shimmon, V. H. Beltran, P. J. Ralph, K. Petrou, Dimethylsulfoniopropionate, superoxide dismutase and glutathione as stress response indicators in three corals under short-term hyposalinity stress. *Proc. R. Soc. B Biol. Sci.* **283**, 20152418 (2016).

26. E. S. Deschaseaux, G. B. Jones, M. A. Deseo, K. M. Shepherd, R. Kiene, H. Swan, P. L. Harrison, B. D. Eyre, Effects of environmental factors on dimethylated sulfur compounds

and their potential role in the antioxidant system of the coral holobiont. *Limnol. Oceanogr.* **59**, 758–768 (2014).

27. C. R. Reisch, M. A. Moran, W. B. Whitman, Bacterial catabolism of dimethylsulfoniopropionate (DMSP). *Front. Microbiol.* **2**, 172 (2011).

28. E. Yoshii, Cytotoxic effects of acrylates and methacrylates: Relationships of monomer structures and cytotoxicity. *J. Biomed. Mater. Res.* **37**, 517–524 (1997).

29. C.-Y. Li, X.-J. Wang, X.-L. Chen, Q. Sheng, S. Zhang, P. Wang, M. Quareshy, B. Rihtman, X. Shao, C. Gao, F. Li, S. Li, W. Zhang, X.-H. Zhang, G.-P. Yang, J. D. Todd, A novel ATP dependent dimethylsulfoniopropionate lyase in bacteria that releases dimethyl sulfide and acryloyl-CoA. *eLife* **10**, e64045 (2021).

30. U. Alcolombri, P. Laurino, P. Lara-Astiaso, A. Vardi, D. S. Tawfik, DddD is a CoA-transferase/lyase producing dimethyl sulfide in the marine environment. *Biochemistry* **53**, 5473–5475 (2014).

31. J. D. Todd, R. Rogers, Y. G. Li, M. Wexler, P. L. Bond, L. Sun, A. R. J. Curson, G. Malin, M. Steinke, A. W. B. Johnston, Structural and regulatory genes required to make the gas dimethyl sulfide in bacteria. *Science* **315**, 666–669 (2007).

32. Y. Cui, S.-K. Wong, R. Kaneko, A. Mouri, Y. Tada, I. Nagao, S.-J. Chun, H.-G. Lee, C.-Y. Ahn, H.-M. Oh, Y. Sato-Takabe, K. Suzuki, H. Fukuda, T. Nagata, K. Kogure, K. Hamasaki, Distribution of dimethylsulfoniopropionate degradation genes reflects strong water current dependencies in the Sanriku coastal region in Japan: From mesocosm to field study. *Front. Microbiol.* **11**, 1372 (2020).

33. J. Liu, C.-X. Xue, J. Wang, A. T. Crombie, O. Carrión, A. W. Johnston, J. C. Murrell, J. Liu, Y. Zheng, X.-H. Zhang, *Oceanospirillales* containing the DMSP lyase DddD are key utilisers of carbon from DMSP in coastal seawater. *Microbiome* **10**, 110 (2022).

34. E. Stackebrandt, B. M. Goebel, Taxonomic note: A place for DNA-DNA reassociation and 16S rRNA sequence analysis in the present species definition in bacteriology. *Int. J. Syst. Evol. Microbiol.* **44**, 846–849 (1994).

35. M. R. Olm, A. Crits-Christoph, S. Diamond, A. Lavy, P. B. Matheus Carnevali, J. F. Banfield, Consistent metagenome-derived metrics verify and delineate bacterial species boundaries. *mSystems* **5**, e00731-19 (2020).

36. M. Kim, H.-S. Oh, S.-C. Park, J. Chun, Towards a taxonomic coherence between average nucleotide identity and 16S rRNA gene sequence similarity for species demarcation of prokaryotes. *Int. J. Syst. Evol. Microbiol.* **64**, 346–351 (2014).

37. R. M. Bowers, N. C. Kyrpides, R. Stepanauskas, M. Harmon-Smith, D. Doud, T. Reddy, F. Schulz, J. Jarett, A. R. Rivers, E. A. Eloe-Fadrosh, S. G. Tringe, N. N. Ivanova, A. Copeland, A. Clum, E. D. Becraft, R. R. Malmstrom, B. Birren, M. Podar, P. Bork, G. M. Weinstock, G. M. Garrity, J. A. Dodsworth, S. Yooseph, G. Sutton, F. O. Glöckner, J. A. Gilbert, W. C. Nelson, S. J. Hallam, S. P. Jungbluth, T. J. G. Ettema, S. Tighe, K. T. Konstantinidis, W.-T. Liu, B. J. Baker, T. Rattei, J. A. Eisen, B. Hedlund, K. D. McMahon, N. Fierer, R. Knight, R. Finn, G. Cochrane, I. Karsch-Mizrachi, G. W. Tyson, C. Rinke; Genome Standards Consortium, A. Lapidus, F. Meyer, P. Yilmaz, D. H. Parks, A M Eren, L. Schriml, J. F. Banfield, P. Hugenholtz, T. Woyke, Minimum information about a single amplified genome (MISAG) and a metagenome-assembled genome (MIMAG) of bacteria and archaea. *Nat. Biotechnol.* **35**, 725–731 (2017).

38. J.-B. Raina, D. M. Tapiolas, S. Forêt, A. Lutz, D. Abrego, J. Ceh, F. O. Seneca, P. L. Clode, D. G. Bourne, B. L. Willis, C. A. Motti, DMSP biosynthesis by an animal and its role in coral thermal stress response. *Nature* **502**, 677–680 (2013).

39. J. M. Gonzalez, J. S. Covert, W. B. Whitman, J. R. Henriksen, F. Mayer, B. Scharf, R. Schmitt, A. Buchan, J. A. Fuhrman, R. P. Kiene, M. A. Moran, *Silicibacter pomeroyi* sp. nov. and *Roseovarius nubinhibens* sp. nov., dimethylsulfoniopropionate-demethylating bacteria from marine environments. *Int. J. Syst. Evol. Microbiol.* **53** (Pt 5), 1261–1269 (2003).

40. U. Karsten, K. Kück, C. Vogt, G. Kirst, "Dimethylsulfoniopropionate production in phototrophic organisms and its physiological functions as a cryoprotectant" in *Biological and environmental chemistry of DMSP and related sulfonium compounds*. (Springer, 1996), pp. 143–153.

41. U. Karsten, G. Kirst, C. Wiencke, Dimethylsulphoniopropionate (DMSP) accumulation in green macioalgae from polar to temperate regions: Interactive effects of light versus salinity and light versus temperature. *Polar Biol.* **12**, 603–607 (1992).

42. T. R. Miller, K. Hnilicka, A. Dziedzic, P. Desplats, R. Belas, Chemotaxis of *Silicibacter* sp. strain TM1040 toward dinoflagellate products. *Appl. Environ. Microbiol.* **70**, 4692–4701 (2004).

43. T. R. Miller, R. Belas, Motility is involved in *Silicibacter* sp. TM1040 interaction with dinoflagellates. *Environ. Microbiol.* **8**, 1648–1659 (2006).

44. M. Landa, A. S. Burns, S. J. Roth, M. A. Moran, Bacterial transcriptome remodeling during sequential co-culture with a marine dinoflagellate and diatom. *ISME J.* **11**, 2677–2690 (2017).

45. J. Li, W. Kuang, L. Long, S. Zhang, Production of quorum-sensing signals by bacteria in the coral mucus layer. *Coral Reefs* **36**, 1235–1241 (2017).

46. W. M. Johnson, M. C. Kido Soule, E. B. Kujawinski, Evidence for quorum sensing and differential metabolite production by a marine bacterium in response to DMSP. *ISME J.* **10**, 2304–2316 (2016).

47. C. Adler, N. S. Corbalan, D. R. Peralta, M. F. Pomares, R. E. de Cristóbal, P. A. Vincent, The alternative role of enterobactin as an oxidative stress protector allows *Escherichia coli* colony development. *PLOS ONE* **9**, e84734 (2014).

48. C. Li, D. Pan, M. Li, Y. Wang, L. Song, D. Yu, Y. Zuo, K. Wang, Y. Liu, Z. Wei, Z. Lui, L. Zhu, Aerobactin-mediated iron acquisition enhances biofilm formation, oxidative stress

resistance, and virulence of *Yersinia pseudotuberculosis*. *Front. Microbiol.* **12**, 699913 (2021).

49. J. S. Wirth, T. Wang, Q. Huang, R. H. White, W. B. Whitman, Dimethylsulfoniopropionate sulfur and methyl carbon assimilation in *Ruegeria* Species. *mBio* **11**, e00329-20 (2020).

50. A. D. Broadbent, G. B. Jones, R. J. Jones, DMSP in corals and benthic algae from the Great Barrier Reef. *Estuar. Coast. Shelf Sci.* **55**, 547–555 (2002).

51. D. M. Tapiolas, J.-B. Raina, A. Lutz, B. L. Willis, C. A. Motti, Direct measurement of dimethylsulfoniopropionate (DMSP) in reef-building corals using quantitative nuclear magnetic resonance (qNMR) spectroscopy. *J. Exp. Mar. Biol. Ecol.* **443**, 85–89 (2013).

52. K. L. Van Alstyne, P. Schupp, M. Slattery, The distribution of dimethylsulfoniopropionate in tropical Pacific coral reef invertebrates. *Coral Reefs* **25**, 321–327 (2006).

53. W. De Coster, S. D'Hert, D. T. Schultz, M. Cruts, C. Van Broeckhoven, NanoPack: Visualizing and processing long-read sequencing data. *Bioinformatics* **34**, 2666–2669 (2018).

54. M. Kolmogorov, D. M. Bickhart, B. Behsaz, A. Gurevich, M. Rayko, S. B. Shin, K. Kuhn, J. Yuan, E. Polevikov, T. P. L. Smith, P. A. Pevzner, MetaFlye: Scalable long-read metagenome assembly using repeat graphs. *Nat. Methods* **17**, 1103–1110 (2020).

55. B. J. Walker, T. Abeel, T. Shea, M. Priest, A. Abouelliel, S. Sakthikumar, C. A. Cuomo, Q. Zeng, J. Wortman, S. K. Young, A. M. Earl, Pilon: An integrated tool for comprehensive microbial variant detection and genome assembly improvement. *PLOS ONE* **9**, e112963 (2014).

56. D. H. Parks, M. Imelfort, C. T. Skennerton, P. Hugenholtz, G. W. Tyson, CheckM: Assessing the quality of microbial genomes recovered from isolates, single cells, and metagenomes. *Genome Res.* **25**, 1043–1055 (2015).

57. A. Marchler-Bauer, S. Lu, J. B. Anderson, F. Chitsaz, M. K. Derbyshire, C. DeWeese-Scott, J. H. Fong, L. Y. Geer, R. C. Geer, N. R. Gonzales, M. Gwadz, D. I. Hurwitz, J. D. Jackson, Z. Ke, C. J. Lanczycki, F. Lu, G. H. Marchler, M. Mullokandov, M. V. Omelchenko, C. L. Robertson, J. S. Song, N. Thanki, R. A. Yamashita, D. Zhang, N. Zhang, C. Zheng, S. H. Bryant, CDD: A Conserved Domain Database for the functional annotation of proteins. *Nucleic Acids Res.* **39** (Suppl 1), D225-D229 (2011).

58. B. Q. Minh, H. A. Schmidt, O. Chernomor, D. Schrempf, M. D. Woodhams, A. von Haeseler, R. Lanfear, IQ-TREE 2: New models and efficient methods for phylogenetic inference in the genomic era. *Mol. Biol. Evol.* **37**, 1530–1534 (2020).

59. S. T. Chambers, C. M. Kunin, D. Miller, A. Hamada, Dimethylthetin can substitute for glycine betaine as an osmoprotectant molecule for Escherichia coli. *J. Bacteriol.* **169**, 4845–4847 (1987).

60. J. S. Wirth, W. B. Whitman, An efficient method for synthesizing dimethylsulfonio-^{34}S-propionate hydrochloride from $^{34}S_8$. *J. Label. Compd. Radiopharm.* **62**, 52–58 (2019).

61. D. Reynolds, T. Thomas, Evolution and function of eukaryotic-like proteins from sponge symbionts. *Mol. Ecol.* **25**, 5242–5253 (2016).

62. M. J. Neave, A. Apprill, C. Ferrier-Pages, C. R. Voolstra, Diversity and function of prevalent symbiotic marine bacteria in the genus *Endozoicomonas*. *Appl. Microbiol. Biotechnol.* **100**, 8315–8324 (2016).

63. C. S. Yang, M. H. Chen, A. B. Arun, C. A. Chen, J. T. Wang, W. M. Chen, *Endozoicomonas montiporae* sp nov., isolated from the encrusting pore coral *Montipora aequituberculata*. *Int. J. Syst. Evol. Microbiol.* **60** (Pt 5), 1158–1162 (2010).

64. M. T. H. D. Nguyen, M. Liu, T. Thomas, Ankyrin-repeat proteins from sponge symbionts modulate amoebal phagocytosis. *Mol. Ecol.* **23**, 1635–1645 (2014).

65. C. Cazalet, C. Rusniok, H. Brüggemann, N. Zidane, A. Magnier, L. Ma, M. Tichit, S. Jarraud, C. Bouchier, F. Vandenesch, F. Kunst, J. Etienne, P. Glaser, C. Buchrieser,

Evidence in the *Legionella pneumophila* genome for exploitation of host cell functions and high genome plasticity. *Nat. Genet.* **36**, 1165–1173 (2004).

66. Z. Stoytcheva, B. Joshi, J. Spížek, P. Tichý, WD-repeat protein encoding genes among prokaryotes of theStreptomyces genus. *Folia Microbiol.* **45**, 407–413 (2000).

67. M. Hisbergues, C. G. Gaitatzes, F. Joset, S. Bedu, T. F. Smith, A noncanonical WD-repeat protein from the cyanobacterium Synechocystis PCC6803: Structural and functional study. *Protein Sci.* **10**, 293–300 (2001).

68. X.-J. Hu, T. Li, Y. Wang, Y. Xiong, X.-H. Wu, D.-L. Zhang, Z.-Q. Ye, Y.-D. Wu, Prokaryotic and highly-repetitive WD40 proteins: A systematic study. *Sci. Rep.* **7**, 10585 (2017).

69. E. J. Neer, C. J. Schmidt, R. Nambudripad, T. F. Smith, The ancient regulatory-protein family of WD-repeat proteins. *Nature* **371**, 297–300 (1994).

70. M. Guo, J. Wang, Y. Zhang, L. Zhang, Increased WD40 motifs in Planctomycete bacteria and their evolutionary relevance. *Mol. Phylogenet. Evol.* **155**, 107018 (2021).

71. D. Laslett, B. Canback, ARAGORN, a program to detect tRNA genes and tmRNA genes in nucleotide sequences. *Nucleic Acids Res.* **32**, 11–16 (2004).

72. T. Seemann, barrnap 0.9: Rapid ribosomal RNA prediction. Google Scholar, (2013).

73. T. Seemann, Prokka: Rapid prokaryotic genome annotation. *Bioinformatics* **30**, 2068–2069 (2014).

74. R. K. Aziz, D. Bartels, A. A. Best, M. DeJongh, T. Disz, R. A. Edwards, K. Formsma, S. Gerdes, E. M. Glass, M. Kubal, F. Meyer, G. J. Olsen, R. Olson, A. L. Osterman, R. A. Overbeek, L. K. McNeil, D. Paarmann, T. Paczian, B. Parrello, G. D. Pusch, C. Reich, R. Stevens, O. Vassieva, V. Vonstein, A. Wilke, O. Zagnitko, The RAST Server: Rapid annotations using subsystems technology. *BMC Genomics* **9**, 75 (2008).

75. R. Overbeek, R. Olson, G. D. Pusch, G. J. Olsen, J. J. Davis, T. Disz, R. A. Edwards, S. Gerdes, B. Parrello, M. Shukla, V. Vonstein, A. R. Wattam, F. Xia, R. Stevens, The SEED and the Rapid Annotation of microbial genomes using Subsystems Technology (RAST). *Nucleic Acids Res.* **42**, D206-D214 (2014).

76. D. Arndt, J. R. Grant, A. Marcu, T. Sajed, A. Pon, Y. Liang, D. S. Wishart, PHASTER: A better, faster version of the PHAST phage search tool. *Nucleic Acids Res.* **44**, W16-W21 (2016).

77. S. Lu, J. Wang, F. Chitsaz, M. K. Derbyshire, R. C. Geer, N. R. Gonzales, M. Gwadz, D. I. Hurwitz, G. H. Marchler, J. S. Song, N. Thanki, R. A. Yamashita, M. Yang, D. Zhang, C. Zheng, C. J. Lanczycki, A. Marchler-Bauer, CDD/SPARCLE: The Conserved Domain Database in 2020. *Nucleic Acids Res.* **48**, D265-D268 (2020).

78. G. Benson, Tandem repeats finder: A program to analyze DNA sequences. *Nucleic Acids Res.* **27**, 573–580 (1999).

79. V. Eichinger, T. Nussbaumer, A. Platzer, M.-A. Jehl, R. Arnold, T. Rattei, EffectiveDB—Updates and novel features for a better annotation of bacterial secreted proteins and Type III, IV, VI secretion systems. *Nucleic Acids Res.* **44**, D669-D674 (2016).

80. E. P. Nawrocki, S. R. Eddy, Infernal 1.1: 100-fold faster RNA homology searches. *Bioinformatics* **29**, 2933–2935 (2013).

81. E. P. Nawrocki, "Annotating Functional RNAs in Genomes Using Infernal" in RNA *Sequence, Structure, and Function: Computational and Bioinformatic Methods*, J. Gorodkin, W. L. Ruzzo, Eds. (Humana Press, 2014), pp. 163–197.

82. S. Kalyaanamoorthy, B. Q. Minh, T. K. F. Wong, A. von Haeseler, L. S. Jermiin, ModelFinder: Fast model selection for accurate phylogenetic estimates. *Nat. Methods* **14**, 587–589 (2017).

83. L.-T. Nguyen, H. A. Schmidt, A. Von Haeseler, B. Q. Minh, IQ-TREE: A fast and effective stochastic algorithm for estimating maximum-likelihood phylogenies. *Mol. Biol. Evol.* **32**, 268–274 (2015).

84. I. Letunic, P. Bork, Interactive Tree Of Life (iTOL) v4: Recent updates and new developments. *Nucleic Acids Res.* **47**, W256-W259 (2019).

85. S. I. Na, Y. O. Kim, S. H. Yoon, S. M. Ha, I. Baek, J. Chun, UBCG: Up-to-date bacterial core gene set and pipeline for phylogenomic tree reconstruction. *J. Microbiol.* **56**, 280–285 (2018).

86. L. Rodriguez-R, K. Konstantinidis. (PeerJ Preprints, 2016).

87. R. C. Team. (2018).

88. R. Kolde, M. R. Kolde, Package 'pheatmap'. R package 1, 790 (2015).

89. W. Shen, S. Le, Y. Li, F. Hu, SeqKit: A cross-platform and ultrafast toolkit for FASTA/Q file manipulation. *PLOS ONE* **11**, e0163962 (2016).

90. J. R. Grant, P. Stothard, The CGView Server: A comparative genomics tool for circular genomes. *Nucleic Acids Res.* **36**, W181-W184 (2008).

91. A. C. Darling, B. Mau, F. R. Blattner, N. T. Perna, Mauve: Multiple alignment of conserved genomic sequence with rearrangements. *Genome Res.* **14**, 1394–1403 (2004).

92. K. Katoh, J. Rozewicki, K. D. Yamada, MAFFT online service: Multiple sequence alignment, interactive sequence choice and visualization. *Brief. Bioinform.* **20**, 1160–1166 (2019).

93. S. Andrews. (Babraham Bioinformatics, Babraham Institute, Cambridge, United Kingdom, 2010).

94. B. Langmead, S. L. Salzberg, Fast gapped-read alignment with Bowtie 2. *Nat. Methods* **9**, 357–359 (2012).

95. Y. Liao, G. K. Smyth, W. Shi, featureCounts: An efficient general purpose program for assigning sequence reads to genomic features. *Bioinformatics* **30**, 923–930 (2014).

96. M. I. Love, W. Huber, S. Anders, Moderated estimation of fold change and dispersion for RNA-seq data with *DESeq2*. *Genome Biol.* **15**, 50 (2014).

97. M. Kanehisa, Y. Sato, K. Morishima, BlastKOALA and GhostKOALA: KEGG tools for functional characterization of genome and metagenome sequences. *J. Mol. Biol.* **428**, 726–731 (2016).

98. S.-H. Yang, C.-H. Tseng, H.-P. Lo, P.-W. Chiang, H.-J. Chen, J.-H. Shiu, H.-C. Lai, K. Tandon, N. Isomura, T. Mezaki, H. Yamamoto, S.-L. Tang, Locality effect of coral-associated bacterial community in the Kuroshio Current from Taiwan to Japan. *Front. Ecol. Evol.* **8**, 569107 (2020).

99. R. Bernasconi, M. Stat, A. Koenders, A. Paparini, M. Bunce, M. J. Huggett, Establishment of coral-bacteria symbioses reveal changes in the core bacterial community with host ontogeny. *Front. Microbiol.* **10**, 1529 (2019).

100. K. Damjanovic, L. L. Blackall, L. M. Peplow, M. J. H. van Oppen, Assessment of bacterial community composition within and among *Acropora loripes* colonies in the wild and in captivity. *Coral Reefs* **39**, 1245–1255 (2020).

101. E. Bolyen, J. R. Rideout, M. R. Dillon, N. A. Bokulich, C. C. Abnet, G. A. Al-Ghalith, H. Alexander, E. J. Alm, M. Arumugam, F. Asnicar, Y. Bai, J. E. Bisanz, K. Bittinger, A. Brejnrod, C. J. Brislawn, C. T. Brown, B. J. Callahan, A. M. Caraballo-Rodríguez, J. Chase, E. K. Cope, R. D. Silva, C. Diener, P. C. Dorrestein, G. M. Douglas, D. M. Durall, C. Duvallet, C. F. Edwardson, M. Ernst, M. Estaki, J. Fouquier, J. M. Gauglitz, S. M. Gibbons, D. L. Gibson, A. Gonzalez, K. Gorlick, J. Guo, B. Hillmann, S. Holmes, H. Holste, C. Huttenhower, G. A. Huttley, S. Janssen, A. K. Jarmusch, L. Jiang, B. D. Kaehler, K. B. Kang, C. R. Keefe, P. Keim, S. T. Kelley, D. Knights, I. Koester, T. Kosciolek, J. Kreps, M. G. I. Langille, J. Lee, R. Ley, Y.-X. Liu, E. Loftfield, C. Lozupone, M. Maher, C. Marotz, B. D. Martin, D. M. Donald, L. J. McIver, A. V. Melnik, J. L.

Metcalf, S. C. Morgan, J. T. Morton, A. T. Naimey, J. A. Navas-Molina, L. F. Nothias, S. B. Orchanian, T. Pearson, S. L. Peoples, D. Petras, M. L. Preuss, E. Pruesse, L. B. Rasmussen, A. Rivers, M. S. Robeson II, P. Rosenthal, N. Segata, M. Shaffer, A. Shiffer, R. Sinha, S. J. Song, J. R. Spear, A. D. Swafford, L. R. Thompson, P. J. Torres, P. Trinh, A. Tripathi, P. J. Turnbaugh, S. Ul-Hasan, J. J. J. van der Hooft, F. Vargas, Y. Vázquez-Baeza, E. Vogtmann, M. von Hippel, W. Walters, Y. Wan, M. Wang, J. Warren, K. C. Weber, C. H. D. Williamson, A. D. Willis, Z. Z. Xu, J. R. Zaneveld, Y. Zhang, Q. Zhu, R. Knight, J. G. Caporaso, Reproducible, interactive, scalable and extensible microbiome data science using QIIME 2. *Nat. Biotechnol.* **37**, 852–857 (2019).

102. R. C. Team, R Core Team R: A language and environment for statistical computing. Foundation for Statistical Computing., (2020).

103. H. Wickham, ggplot2. *Wiley interdisciplinary reviews: computational statistics* **3**, 180–185 (2011).